

ANALYTICAL AND EXPERIMENTAL INVESTIGATION OF THE DYNAMIC RESPONSE OF LIQUID-FILLED CONICAL TANKS

A EL DAMATTY¹, R M KOROL² And L M TANG³

SUMMARY

Conical steel vessels are commonly used as water containment for elevated tanks. One of the phenomena associated with the seismic response of liquid-filled tanks is the sloshing motion occurring at the top free surface. In this paper, a mathematical model is developed to predict the liquid sloshing frequencies and corresponding mode shapes of liquid-filled conical tanks subjected to seismic motion. A shake table testing program for a small-scaled conical tank was also conducted to calibrate the mathematical model. This leads to the develop of four equations that can be used to predict the free vibration of the sloshing motion.

INTRODUCTION

An elevated steel conical tank that is anchored to a reinforced concrete shaft rising above the sky-line is becoming very widely used as a water storage structure in many communities around the world. Fig. 1 shows a typical “pure” conical tank photographed in Guang Dong Province, China, whereas in North America, the “composite” type that combines a cone and cylinder segment on the top, are common. This paper will focus on the “pure” conical-shaped structure.

El Damatty et al (1997a and b) have studied the stability of such structures when subjected to a combination of hydrostatic pressure and seismic excitation. The effect of the impulsive component of the dynamic pressure was accounted for in this earlier work, but the sloshing effect of the contained fluid was not considered. To our knowledge, the current study represents the first attempt to study the sloshing response of conical tanks. An analytical model has been developed to predict the natural frequencies and corresponding mode shapes for the sloshing motion. A shaking table testing program for small-scaled conical tanks, intended to model the response of prototype structures was also conducted to calibrate the model.

ANALYTICAL METHOD

In deriving the fluid equations of motion, the following assumptions were imposed:

- 1) the fluid's displacements are small and therefore linear theory is applicable,
- 2) the fluid is assumed to be incompressible, inviscid, and irrotational, i.e. an ideal fluid,
- 3) decoupling exists between the sloshing motion and the shell vibrations.

The validity of the decoupling between the sloshing and the shell vibration is reasonable, since for prototype structures the sloshing fundamental frequency will be much lower than for that for the tank walls.

¹ Department of Civil Engineering, University of Western Ontario, Canada

² Department of Civil Engineering, McMaster University, Canada

³ Department of Civil Engineering, McMaster University, Canada

The coordinate system used, together with the notations for the dimensions, are defined in Fig. 2. The velocity potential ϕ is a scalar function whose derivative with respect to a specified direction leads to the velocity of the fluid along that direction. For an ideal fluid, then, Laplace's equation applies, such that

$$\nabla^2 \phi = \frac{\partial^2 \phi}{\partial r^2} + \frac{1}{r} \frac{\partial \phi}{\partial r} + \frac{1}{r^2} \frac{\partial^2 \phi}{\partial \theta^2} + \frac{\partial^2 \phi}{\partial z^2} = 0 \quad (1)$$

for $R_1 < r < R$ and $0 < z < H$.

The sloshing motion natural frequencies and their corresponding mode shapes can be found by solving Eq. (1) together with a set of homogeneous boundary conditions. These are:

$$\frac{\partial \phi}{\partial z}(r, \theta, z, t) = 0 \quad (\text{at } z = 0)$$

(2)

$$\frac{\partial \phi}{\partial n} = \frac{\partial \phi}{\partial r} \cos \beta - \frac{\partial \phi}{\partial z} \sin \beta = 0; \quad (\text{at } r = R_1 + z \tan \beta)$$

(3)

$$\frac{\partial^2 \phi}{\partial t^2}(r, \theta, z, t) + g \frac{\partial \phi}{\partial z}(r, \theta, z, t) = 0; \quad (\text{at } z = H)$$

(4)

where t is time, g is the gravitational constant, and other variables are defined in Fig. 2. Using the method of separation of variables, the velocity potential, ϕ , can be expressed as:

$$\phi = R(r) \theta(\theta) Z(z) T(t)$$

(5)

where R , Z , and T represent single variable functions of the coordinates noted. Substituting equation (5) into Eq. (1) results in a group of three second order ordinary differential equations involving the functions θ , Z , and R , the solutions of which are:

$$\theta_{(\theta)} = B_1 \sin(m\theta) + B_2 \cos(m\theta)$$

$$(6) \quad Z_{(z)} = A_1 \cosh(kz)$$

(7)

$$R_{(r)} = C_{1m} J_m(kr) + D_m I_m(kr)$$

(8)

Here, A_1 , B_1 , B_2 , C_m and D_m are constants, while $J_m(kr)$ and $I_m(kr)$ are the first and modified second kind Bessel functions respectively. The sloshing modes of interest are those due to horizontal excitation; they vary in a $\cos \theta$ manner so that the solution of Laplace's equation (1) will be given by:

$$\phi(r, \theta, z, t) = \left\{ \sum_{i=1}^{\infty} [A_i(t) I(k_i r) \cos(k_i z)] + \sum_{j=1}^{\infty} [B_j(t) J(k_j r) \cosh(k_j z)] \right\} \cos \theta$$

(9)

The impulsive component is represented by the first term, while the second term, ϕ_s , represents the effect of free surface motion (sloshing). To solve for the frequencies and mode shapes for the sloshing effect, ϕ_s is substituted into the homogeneous boundary condition of the tank wall, which is expressed by Eq. (3), give to the following equation that can be used to obtain the k_i :

$$\sum_{j=1}^{\infty} [B_{j(t)} J'(k_j r) \cosh(k_j z)] \cos \theta \cos \beta - \sum_{j=1}^{\infty} [B_{j(t)} J(k_j r) \sinh(k_j z)] \cos \theta \sin \beta = 0$$

(10)

$$\text{at } r = R_1 + z \tan \beta$$

As such, for each separate mode j , the k_j can be obtained from the solution of the following equation:

$$J'(k_j r) \cosh(k_j z) \cos \beta - k J(k_j r) \sinh(k_j z) \sin \beta = 0$$

(11)

$$\text{at } r = R_1 + z \tan \beta$$

Once this is done, its value can be substituted into the free surface boundary condition given by Eq. (4). The result is a second order differential equation that allows for the solution of the natural sloshing frequency ω_j given by:

$$\omega_j^2 = g k_j \tanh(k_j H)$$

(12)

while the mode shape is determined by

$$\delta = J(k_j r) \cosh(k_j z)$$

(13)

It is of interest to note that while k_j is a constant for the cylindrical tank solution, it is a function of z for the cone. Now, for a given geometry of conical tank and water depth, the variation of k_j can be plotted for different modes of vibration. In the case of a small scale model (1:80), plots are shown in Fig. 3 for k_1 and k_2 for the first two modes with water elevation $z <$ the depth H . In this instance, the tank model had a bottom radius $R_1 = 0.05\text{m}$, a water depth $H = 0.10\text{m}$ and an angle of inclination of the cone generators of $\beta = 45^\circ$. It is evident that the variation of k_j with z is quite small at the top part of the tank. This is to be expected since the top region of the tank would mostly influence the sloshing response.

The variation of k_j (also for the first and second modes) for a prototype tank having a bottom radius of 4.0m and a height $H = 8.0\text{m}$ is shown in Fig. 4. From this figure, it is evident that the trend of the variation of k_j for the prototype conical tank is very similar to the reduced-scale model variation, however, the values for k_j are much less. The reason for the difference will be discussed subsequently.

SHAKE TABLE TEST ON MODEL CONE

Shake table tests were conducted on a small scale tank model, the size of which relates to the description of Fig. 3. The purpose was to evaluate experimentally the sloshing natural frequencies and mode shapes, and compare the observed response with that predicted by the mathematical model. The model was fabricated from a steel sheet of 1.5mm thickness. A $0.20\text{m} \times 0.30\text{m}$ steel base-plate was welded to the bottom of the tank which was in turn bolted to the shake table.

Steady state sinusoidal accelerations having various frequencies were input to the shake table on which the tank model was mounted, with tests conducted on the model structure with water levels of different depths. Initially, the water depth had to be specified. Since the first and second modes are the most important, a determination of the first two natural frequencies would be of paramount interest.

To assess the natural frequencies of sloshing, a wide range of input frequencies was applied starting from the low range and working up the scale. In the vicinity of a natural frequency, the vibration of the free surface becomes noticeable. A frequency sweep test in the vicinity of the desired value was done to determine it accurately.

For each input excitation, (fa), the variation in the water displacement, w , of a point located on the free surface was recorded. This was done once steady-state response of the fluid was achieved. In addition, the variation of the acceleration at the water surface was also recorded using an accelerometer. To eliminate the effect of any higher modes in both the input acceleration and the output fluid displacement, a Fast Fourier Transform (FFT) was done on both records. This leads to an evaluation of the input power density for the acceleration $a(fa)$ and the output power density for the displacement $w(fa)$ both expressed in the frequency domain.

Results of the Test ($H = 0.10\text{m}$) and Comparison with Mathematical model

A convenient way of determining a natural frequency value is to plot the ratio between the output and the input density function, $R(fa)$, corresponding to the input excitation, against the applied input frequency. When the maximum R is reached, the value of applied frequency becomes equal to one of the natural frequencies.

Therefore, after determining that the first mode frequency was between 1.22 and 1.39 Hz, a sweep test was done. A plot of $R(fa)$ and the applied frequencies fa is shown in Fig. 5(a). The peak response occurred when the applied frequency was 1.31 Hz. This value is the lowest natural frequency.

The second mode frequency was determined in a similar way. A plot of the second mode $R(fa)$ vs fa curve is shown in Fig. 6(a). In this case the frequency was observed to be about 2.8 Hz.

As previously mentioned, the purpose of the experimental program conducted in this study was to calibrate the mathematical model that was derived earlier in this paper. The main objective is to suggest a depth “z”, at which the coefficient “k” can be calculated using Eq. (11), that would provide a good estimate for the sloshing natural frequencies. A comparison is carried out between the experimentally evaluated sloshing frequencies and those evaluated from the mathematical model using different “k” values.

The values of the first two natural frequencies f_1 and f_2 evaluated from the mathematical model using three different approaches are presented in Table 1. These three approaches are described below:

- 1) The coordinate “z” is equal to the total height of the fluid “H” and substituted into Eq. (11) in order to obtain k_j (for $j = 1$ and 2) that corresponds to the water surface.
- 2) The surface of the tank is divided to a large number of segments. The coordinate “z” of each segment is substituted into Eq. (11) to obtain the equivalent $k_j(z)$. The average value for k_j is then evaluated as follows:

$$\bar{k}_j = \frac{\sum_{i=1}^N k_j(z)}{N}$$

where N is the total number of segments.

- 3) In this approach, a mass weighted average is used to estimate “k”. The surface of the tank is divided into “N” segments similar to Approach 2. The mass of the fluid “ dm ” corresponding to each segment is evaluated. The mass weighted average k_j is then evaluated as follows:

$$\bar{k}_j = \frac{\sum_{i=1}^N k_j(z)dm}{M}$$

where M is the total mass of the fluid inside the tank.

The values of k_j ($j = 1, \text{and } 2$) corresponding to the three approaches are given in Table 1. For each “ k_j ”, a corresponding natural frequency “ f_j ” is then evaluated using Eq. (12). In the same table, the ratios between “ f_j ” evaluated mathematically (using the three approaches) to the corresponding “ f_j ” obtained from the test results are presented. The following observations can be drawn from Table 1.

- 1) “k” based on the water surface (approach 1) underestimates the frequency of the first mode by about 20%. However, the value of “k” based on this approach provides a very good estimate for the second mode frequency.
- 2) “k” based on the average value (approach 2) overestimates the natural frequencies for both the first and second modes by values varying between 26% and 40%.
- 3) “k” based on the mass weighted average consistently overestimates the natural frequencies (for the first and second mode) by values varying between 13% and 15%.

Due to space limitation, only one test was reported in this paper. Results of the three other tests are reported by Tang (1999). A Similar trend of results was obtained from the other three tests. In the same study Tang (1999), plots of the first and second mode shapes at the free surface that resulted from the test and the mathematical model were given. These plots showed an excellent agreement between the test and the mathematical model.

CONCLUSION

This study includes the development of a mathematical model that can predict the natural frequency and mode shape of sloshing motion in conical tanks. The comparison between shaking table test results and the mathematical model indicates that if the natural frequency is evaluated using a mass weighted average value for coefficient “k”, the calculated value will be within 15% of the real one.

REFERENCE

1. Aslam M., Godden W. G. and Theodore S. D. (1979), “ Earthquake Sloshing in Annular and Cylindrical Tanks”, *Journal of the Engineering Mechanics Division* Vol. 105, No.EM3.
2. EI Damatty A., Mirza F. A. and Korol R. M. (1997a), “Stability of Imperfect Steel Conical Tanks under Hydrostatic Loading”, *J. Struct.Engng. ASCE* 123, 703-712.
3. EI Damatty A., Mirza F. A. and Korol R. M. (1997b), “Stability of Elevated Liquid-Filled Conical Tanks under Seismic Loading, Part I—Theory”, *Earthquake Engng. Struct. Dyn.* 26, 1191—1208.
4. EI Damatty A., Mirza F. A. and Korol R. M. (1997c), “Stability of Elevated Liquid-Filled Conical Tanks under Seismic Loading, Part II—Application”, *Earthquake Engng. Struct. Dyn.* 26, 1209—1229.
5. Housner G. W. (1957), “Dynamic Pressures on Accelerated Fluid Containers”. *Bulletin Seism. Soc. America*, Vol. 47, No.1, pp.15-35.
6. Haroun M. A. (1980), “Dynamic Analyses of Liquid Storage Tanks”, EERL Report No. 80-04, California Institute of Technology, Pasadena, CA.
7. Tang L. M. (1999), “Dynamic Behavior of Liquid-Filled Cylindrical and Conical Tanks”, Master Thesis, McMaster University, Hamilton, Ontario, Canada.

Table 1: comparison between the analytical results and experimental results for model cone

	Water Depth = 0.1m					
	First Mode			Second Mode		
	K1	f1	Ratio	K2	f2	Ratio
Experimental Results	9.39	1.31		31.66	2.8	
Analytical "k" Based on Water Surface	7.303	1.08	0.82	30.48	2.74	0.98
Analytical "k" Based on Average	13.92	1.75	1.33	50.3	3.53	1.26
Analytical "k" Based on Mass Weighted Average	10.96	1.48	1.13	42.05	3.23	1.15

Ratio = $f(\text{analytical}) / f(\text{experiment})$



Figure1: A Typical "Pure" Conical Tank

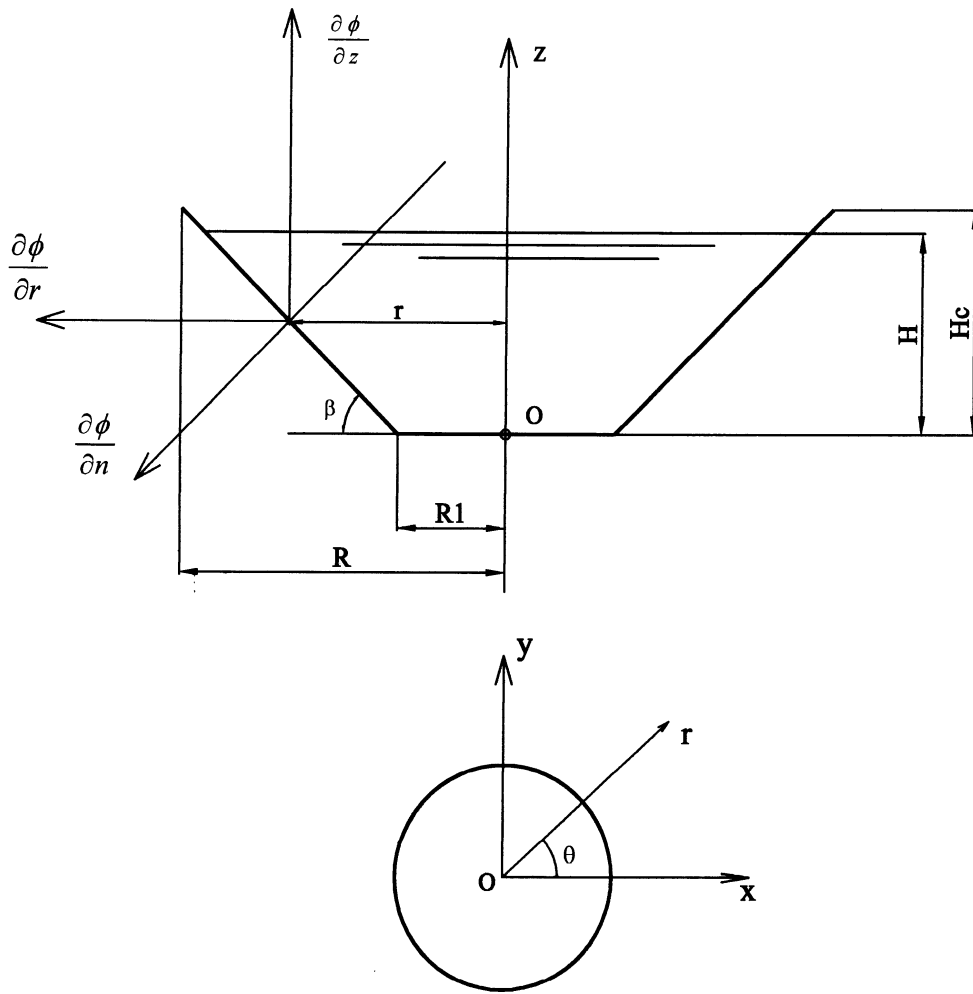


Figure2 : The Coordinate System of Conical Tank

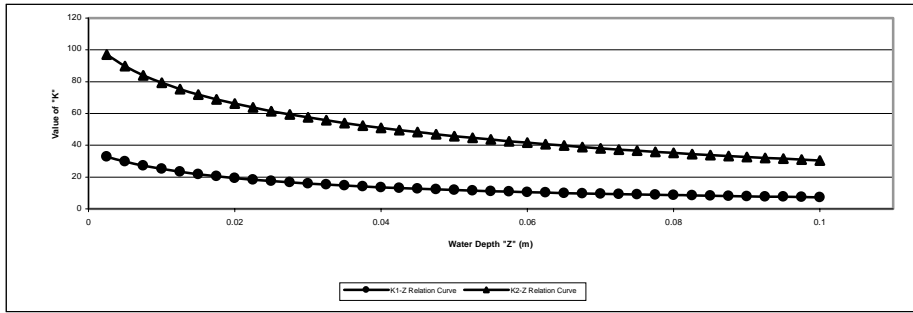


Figure 3: The Relation Between "K" and Water Depth "Z" for Small-Scaled Pure Conical Tank ($R1=0.05m$, $Hc=0.15m$)

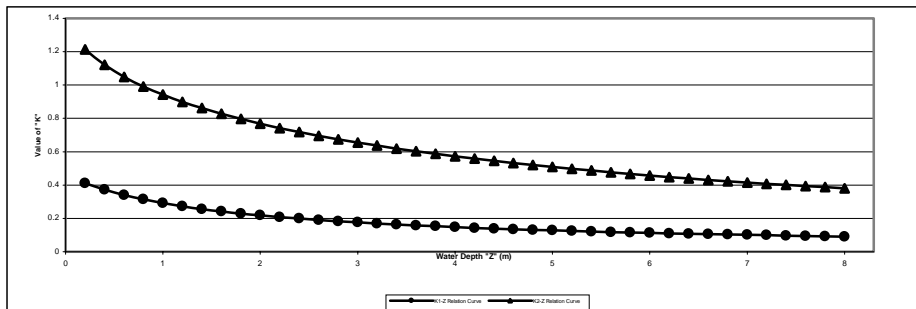


Figure 4: The Relation Between "K" and Water Depth "Z" for Prototype Pure Conical Tank ($R1=4m$, $Hc=8m$)

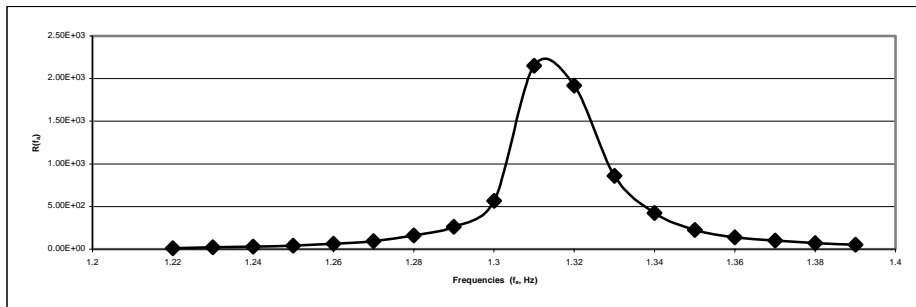


Figure 5: Normalized Output Power Density Distribution (First Mode, Water Depth=0.1m)

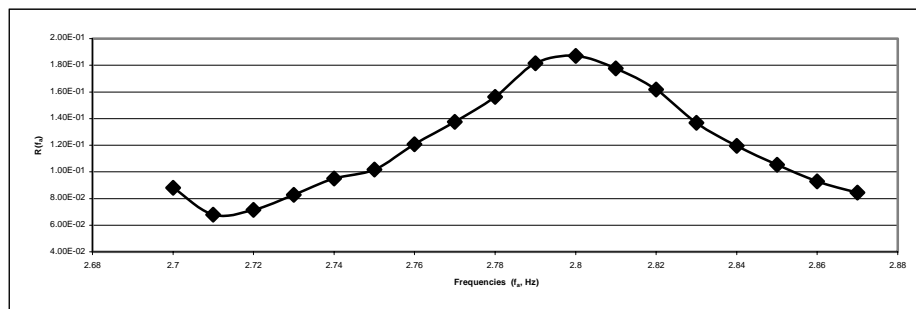


Figure 6: Normalized Output Power Density Distribution (Second Mode, Water Depth=0.1m)